MOLECULAR AND CELLULAR BIOLOGY, May 2002, p. 3292–3300 Vol. 22, No. 10
0270-7306/02/$04.00+0 DOI: 10.1128/MCB.22.10.3292–3300.2002
Copyright © 2002, American Society for Microbiology. All Rights Reserved.

c-Abl Tyrosine Kinase Regulates the Human Rad9 Checkpoint Protein in Response to DNA Damage

Kiyotsugu Yoshida,[1] Kiyoshi Komatsu,[2] Hong-Gang Wang,[2] and Donald Kufe[1]*

Dana-Farber Cancer Institute, Harvard Medical School, Boston, Massachusetts 02115,[1] and Drug Discovery Program, H. Lee Moffitt Cancer Center and Research Institute, University of South Florida College of Medicine, Tampa, Florida 33612[2]

Received 19 November 2001/Returned for modification 8 January 2002/Accepted 12 February 2002

The ubiquitously expressed c-Abl tyrosine kinase is activated in the apoptotic response of cells to DNA damage. The mechanisms by which c-Abl signals the induction of apoptosis are not understood. Here we show that c-Abl binds constitutively to the mammalian homolog of the *Schizosaccharomyces pombe* Rad9 cell cycle checkpoint protein. The SH3 domain of c-Abl interacts directly with the C-terminal region of Rad9. c-Abl phosphorylates the Rad9 Bcl-2 homology 3 domain (Tyr-28) in vitro and in cells exposed to DNA-damaging agents. The results also demonstrate that c-Abl-mediated phosphorylation of Rad9 induces binding of Rad9 to the antiapoptotic Bcl-x_L protein. The regulation of Rad9 by c-Abl in the DNA damage response is further supported by the demonstration that the interaction between c-Abl and Rad9 contributes to DNA damage-induced apoptosis. These findings indicate that Rad9 is regulated by a c-Abl-dependent mechanism in the apoptotic response to genotoxic stress.

The *Schizosaccharomyces pombe* checkpoint proteins spRad1, spHus1, and spRad9 are essential for cell cycle arrest in the presence of incomplete DNA replication or DNA damage (3, 4). Identification of the human homologs hRad1, hHus1, and hRad9 has provided support for conservation of this checkpoint signaling pathway (14, 29, 32, 38, 48). Also, as shown for yeast, hRad9 forms a complex with hRad1 and hHus1 (45, 50). Nuclear hRad9 is constitutively detectable as multiple phosphorylated forms (45). Other studies have demonstrated that hRad9 is phosphorylated in response to DNA damage (50) and that hRad9 localizes to extraction-resistant nuclear complexes in the presence of DNA lesions (7). Recombinant hRad9 has been shown to exhibit 3′-5′ exonuclease activity (6). Moreover, the finding that Rad9 interacts with the antiapoptotic Bcl-2 and Bcl-x_L proteins has supported a role for Rad9 in the apoptotic response to DNA damage (26, 27).

The ubiquitously expressed c-Abl tyrosine kinase is activated in the response to DNA damage (23). Nuclear c-Abl interacts with the DNA-dependent protein kinase (DNA-PK)/Ku complex (17, 19). Phosphorylation of c-Abl by the catalytic subunit DNA-PKcs induces c-Abl activity (19). Other work has demonstrated that c-Abl is activated by the product of the gene mutated in ataxia telangiectasia (ATM) (5, 44). Activation of nuclear c-Abl by DNA damage contributes to induction of apoptosis by mechanisms in part dependent on the p53 tumor suppressor and its homolog p73 (2, 15, 54, 57, 58). Nuclear c-Abl also contributes to DNA damage-induced activation of the c-Jun N-terminal kinase/stress-activated protein kinase (SAPK) and p38 mitogen-activated protein kinase pathways (20, 22, 23, 37). In addition, the finding that c-Abl interacts with the Rad51 protein in response to DNA damage has supported a role for c-Abl in coordinating recombinational DNA repair with the induction of apoptosis (56).

The present studies demonstrate that c-Abl interacts with Rad9 in cells exposed to DNA-damaging agents. c-Abl phosphorylates Rad9 on Y28 in the Bcl-2 homology 3 (BH3) domain and induces binding of Rad9 to Bcl-x_L. The results also demonstrate that c-Abl regulates the apoptotic response to genotoxic stress by a Rad9-dependent mechanism.

MATERIALS AND METHODS

Cell culture. Human U-937 myeloid leukemia cells (American Type Culture Collection [ATCC]) and U-937 cells overexpressing Bcl-x_L (U-937/Bcl-x_L) (9) were cultured in RPMI 1640 medium supplemented with 10% heat-inactivated fetal bovine serum (FBS), 100 U of penicillin/ml, 100 μg of streptomycin/ml, and 2 mM L-glutamine. 293T embryonal kidney cells (ATCC), HeLa cells (ATCC), wild-type (c-*abl*$^{+/+}$) murine embryo fibroblasts (MEFs), c-*abl*$^{-/-}$ MEFs (23, 47), and c-*abl*$^{-/-}$ MEFs expressing c-Abl (c-*abl*$^{+}$) (23) were grown in Dulbecco's modified Eagle's medium containing 10% FBS and antibiotics. Cells were treated with 10 μM ara-C (Sigma-Aldrich). Irradiation was performed at room temperature with a Gammacell 1000 (Atomic Energy of Canada) and a ^{137}Cs source emitting at a fixed rate of 0.21 Gy/min. In certain experiments, cells were pretreated with 1 μM STI-571 (Novartis Pharma AG) (11) for 24 h and then exposed to ara-C or radiation.

Plasmid construction. The vector expressing green fluorescent protein (GFP)-Rad9 has been described (27). The Rad9(Y28-F) variant was generated by site-directed mutagenesis, and the mutation was confirmed by DNA sequencing. Rad9 (1-265) and Rad9 (266-391) were generated by PCR. The Rad9 cDNAs were subcloned into the pHM6 (hemagglutinin [HA] tagged; Roche Molecular Biochemicals), pLXSN (Clontech), pGEX4T-1 (Pharmacia Biotech), and pET-28a (Novagen) vectors.

Cell transfections and infections. 293T cells were transiently transfected by the calcium phosphate method. The total DNA concentration was kept constant by including an empty vector. For retrovirus infections, PG13 cells (34) were transiently transfected with pLXSN-Rad9 or pLXSN-Rad9(Y28-F) by the Superfect transfection kit (Qiagen). At 48 h posttransfection, filtered supernatants with Polybrene (Sigma-Aldrich) were added to the MEFs.

Immunoprecipitation and immunoblot analysis. Cell lysates were prepared as described previously (52, 53) and cleared by centrifugation at 12,000 × *g* for 15 min. Soluble proteins (500 μg) were incubated with anti-Rad9 (sc-8324; Santa-Cruz Biotechnology [SCBT]), anti-c-Abl (sc-131; SCBT), anti-HA (Roche Molecular Biochemicals), or anti-GFP (Roche Molecular Biochemicals) for 2 to 6 h at 4°C, followed by incubation with protein A/G-Sepharose beads (SCBT) for 1 h. The immune complexes and cell lysates (50 μg) were subjected to immu-

* Corresponding author. Mailing address: Dana-Farber Cancer Institute, Harvard Medical School, Boston, MA 02115. Phone: (617) 632-3141. Fax: (617) 632-2934. E-mail: donald_kufe@dfci.harvard.edu.

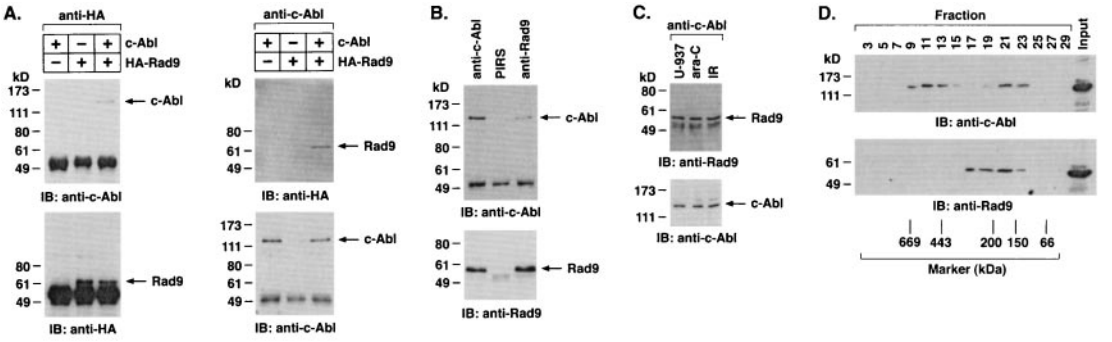

FIG. 1. Association of c-Abl with Rad9. (A) 293T cells were transfected with 3 μg of pSRαMSV/c-Abl and/or pHM6/Rad9. Transfection efficiency as determined with pcDNA3-LacZ and β-galactosidase staining was 81.7% ± 9.2% (mean ± standard deviation of three independent experiments). Cell lysates were immunoprecipitated with anti-HA (left) or anti-c-Abl (right). Immune complexes were subjected to immunoblotting (IB) with anti-c-Abl and anti-HA. (B) Lysates from U-937 cells were immunoprecipitated with preimmune rabbit serum (PIRS), anti-c-Abl, or anti-Rad9. The precipitates were subjected to immunoblotting with anti-c-Abl (top) or anti-Rad9 (bottom). (C) U-937 cells were treated with 10 μM ara-C or 15 Gy of IR and collected at 2 h. Anti-c-Abl immunoprecipitates were analyzed by immunoblotting with anti-Rad9 (top) or anti-c-Abl (bottom). (D) Nuclear extracts from U-937 cells were layered onto a 10 to 35% glycerol gradient. After fractionation, the indicated fractions were subjected to SDS-PAGE and immunoblotting with anti-c-Abl (top) or anti-Rad9 (bottom).

noblot analysis with anti-Rad9 (Transduction Laboratories), anti-c-Abl (Ab-3; Oncogene Research Products), anti-HA, anti-GFP, anti-glutathione *S*-transferase (GST; Upstate Biotechnology Inc.), anti-P-Tyr (4G10; Upstate Biotechnology), or anti-Bcl-x_L (21). The antigen-antibody complexes were visualized by chemiluminescence (NEN Life Science Products). Intensity of the signals was quantitated by densitometric scanning and analysis with the ImageQuant program (Molecular Dynamics, Sunnyvale, Calif.).

Glycerol gradient sedimentation analysis. Nuclear extracts from U-937 and U-937/Bcl-x_L cells were prepared as described previously (10). Two hundred microliters of nuclear extracts was layered on a 10 to 35% glycerol gradient (5 ml) formed in a solution containing 50 mM Tris-HCl [pH 7.3], 0.1 M KCl, 0.2 mM EDTA, 10 mM β-mercaptoethanol, and 0.1% NP-40. After centrifugation at 250,000 × *g* for 12 h at 4°C, fractions (150 μl) were collected from the bottom of the tube. Equal volumes (20 μl) of each sample were analyzed by sodium dodecyl sulfate-polyacrylamide gel electrophoresis (SDS-PAGE) and immunoblotting with anti-c-Abl, anti-Rad9, or anti-Bcl-x_L. As controls, protein standards (Sigma) were separated under identical conditions.

In vitro binding assays. Cell lysates were incubated with purified GST, GST–c-Abl SH2, and GST–c-Abl SH3 (58) in lysis buffer for 2 h at 4°C. The adsorbates were analyzed by immunoblotting with anti-Rad9 or anti-GST. For direct binding assays, GST, GST–c-Abl, and GST–c-Abl SH3 (58) were incubated with purified His-Rad9, His-Rad9 (1-265), or His-Rad9 (266-391) for 1 h at 4°C. The complexes were subjected to immunoblot analysis with anti-Rad9 or anti-His (SC803; SCBT).

In vitro kinase assays. A recombinant c-Abl protein was purified from Sf9 cells infected with a baculovirus vector expressing GST–c-Abl or GST–c-Abl(K-R). The procedure for purifying GST–c-Abl with glutathione beads was as described previously (33) and as modified by our laboratory (22). Purity of the recombinant protein was ≥90% as determined by SDS-PAGE and Coomassie brilliant blue staining. GST–c-Abl, GST–c-Abl(K-R), and c-Abl with the SH3 domain deleted (c-AblΔSH3; Oncogene) were incubated in kinase buffer (50 mM HEPES [pH 7.4], 10 mM $MgCl_2$, 10 mM $MnCl_2$, 2 mM dithiothreitol, 0.1 mM sodium vanadate) with purified GST-Rad9, GST-Rad9(Y28-F), GST-Rad9 (1-265), or GST-Crk (120-225) and [γ-^{32}P]ATP (3,000 Ci/mmol; NEN Life Science Products) for 15 min at 30°C. Phosphorylated proteins were separated by SDS-PAGE and analyzed by autoradiography.

In vitro Rad9/Bcl-x_L complex assays. GST, GST-Rad9, GST-Rad9(Y28-F), and GST-Rad9 (1-265) were incubated in kinase buffer with or without purified c-Abl and ATP for 30 min at 30°C and then coincubated with His–Bcl-x_L (21) in lysis buffer for 1 h at 4°C. Adsorbates to glutathione beads and the residual supernatants were subjected to immunoblotting with anti-Bcl-x_L.

Apoptosis assays. DNA content was assessed by staining ethanol-fixed cells with propidium iodide and monitoring by FACScan (Becton Dickinson). The numbers of cells with sub-G_1 DNA were determined with a CellQuest program (Becton Dickinson).

RESULTS

c-Abl associates with Rad9. To investigate whether c-Abl associates with Rad9, lysates from 293T cells cotransfected with c-Abl and a HA epitope-tagged Rad9 (HA-Rad9) were subjected to immunoprecipitation with an anti-HA antibody. Analysis of the immunoprecipitates with anti-c-Abl showed binding of c-Abl and Rad9 (Fig. 1A, left). The reciprocal experiment, in which anti-c-Abl immunoprecipitates were analyzed by immunoblotting with anti-HA, confirmed coimmunoprecipitation of c-Abl and Rad9 (Fig. 1A, right). Similar findings were obtained with HeLa cells cotransfected with c-Abl and Rad9 (data not shown). To assess whether endogenous c-Abl associates with endogenous Rad9, anti-c-Abl immunoprecipitates from U-937 cells were subjected to immunoblotting with anti-Rad9. The results demonstrate constitutive binding of endogenous c-Abl and Rad9 (Fig. 1B). Immunoblot analysis of anti-Rad9 immunoprecipitates with anti-c-Abl provided further support for constitutive binding of the endogenous c-Abl and Rad9 proteins (Fig. 1B). To determine whether DNA damage affects the binding of c-Abl and Rad9, U-937 cells were treated with ara-C or ionizing radiation (IR). Analysis of anti-c-Abl immunoprecipitates with anti-Rad9 demonstrated little if any change in c-Abl–Rad9 complexes for ara-C-treated, compared to control, cells (Fig. 1C). Similar results were obtained with IR-treated cells (Fig. 1C). To confirm the constitutive binding of c-Abl and Rad9, nuclear lysates from U-937 cells were subjected to sedimentation in a glycerol gradient. Analysis of the gradient fractions by immunoblotting with anti-c-Abl and anti-Rad9 demonstrated cosedimentation of c-Abl and Rad9 in fractions 19 to 23 (Fig. 1D). These findings collectively demonstrate that c-Abl associates with Rad9 in cells and that constitutive binding is not affected by DNA damage.

To further define the association of c-Abl and Rad9, lysates from U-937 cells were incubated with GST fusion proteins containing the c-Abl SH2 or SH3 domain. Analysis of the adsorbates with anti-Rad9 showed binding of Rad9 to GST–c-Abl SH3 but not to GST or GST–c-Abl SH2 (Fig. 2A). The

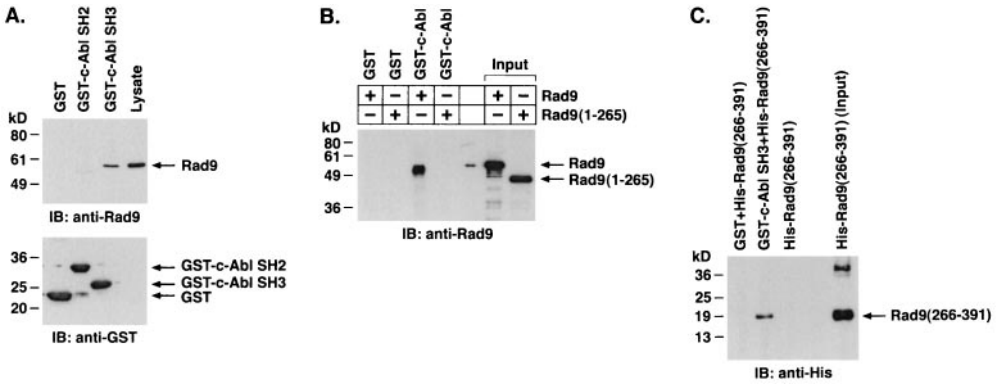

FIG. 2. c-Abl binds directly to Rad9. (A) U-937 cell lysates were incubated with GST, GST–c-Abl SH2, or GST–c-Abl SH3 bound to glutathione beads. The adsorbates were analyzed by immunoblotting (IB) with anti-Rad9 (top) or anti-GST (bottom). (B) Column-purified His-Rad9 and His-Rad9 (1-265) were incubated with glutathione beads containing GST or GST–c-Abl. The adsorbates were analyzed by immunoblotting with anti-Rad9. (C) His-Rad9 (266-391) was incubated with GST or GST–c-Abl SH3 bound to glutathione beads. The adsorbates were subjected to immunoblot analysis with anti-His.

identification of several potential sequences for c-Abl SH3 binding (12, 40) in the Rad9 C-terminal proline-rich region (PQPP, amino acids 331 to 334; PKSP, amino acids 334 to 337; PGTP, amino acids 353 to 356; PQGP, amino acids 376 to 379) suggested that there is a direct interaction between these two proteins. To assess involvement of the Rad9 C-terminal region in binding to c-Abl, a His-tagged Rad9 (1-265) fusion protein with a deletion of the C-terminal 126 amino acids was generated. The association of His-Rad9(full length [FL]), but not His-Rad9 (1-265), with purified GST–c-Abl indicated that c-Abl binds directly to the C-terminal region of Rad9 (Fig. 2B). In addition, the finding that GST–c-Abl SH3, and not GST, binds to His-Rad9 (266-391) provided further support for the direct binding of the c-Abl SH3 domain to the Rad9 C-terminal region (Fig. 2C).

Rad9 Y-28 is required for c-Abl phosphorylation. To assess whether c-Abl phosphorylates Rad9, we incubated purified kinase-active c-Abl, kinase-inactive c-Abl(K-R), and c-AblΔSH3 with GST-Rad9 and [γ-^{32}P]ATP. Analysis of the products by SDS-PAGE and autoradiography showed that Rad9 is a substrate for c-Abl but not c-Abl(K-R) in vitro (Fig. 3A). The finding that phosphorylation of Rad9 by c-AblΔSH3 is decreased compared to that obtained with full-length c-Abl indicates that the binding of the c-Abl SH3 domain facilitates Rad9 phosphorylation (Fig. 3A). Rad9 contains a BH3 domain but not other BH domains that are characteristic of the Bcl-2 family (27). Conserved BH3 domains within proapoptotic proteins are critical for binding to and neutralizing the activity of anti-apoptotic Bcl-2 family members (1, 18). A Y28ELP site in the Rad9 BH3 domain is a consensus sequence for c-Abl phosphoryla-

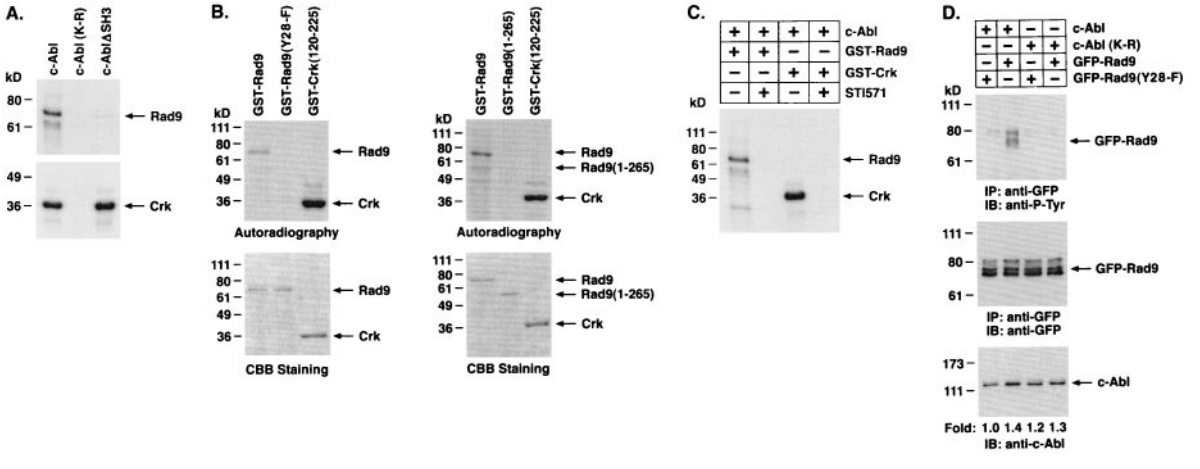

FIG. 3. c-Abl phosphorylates Rad9 on tyrosine 28. (A) Recombinant c-Abl, c-Abl(K-R), and c-Abl with SH3-deleted (c-AblΔSH3) were incubated with [γ-^{32}P]ATP and GST-Rad9 (top) or GST-Crk (120-225) (bottom). The reaction products were analyzed by SDS-PAGE and autoradiography. (B) GST-Rad9, GST-Rad9(Y28-F) (left), and GST-Rad9 (1-265) (right) were incubated with recombinant c-Abl and [γ-^{32}P]ATP. GST-Crk (120-225) was used as a positive control. The reaction products were analyzed by SDS-PAGE and autoradiography (top) or Coomassie brilliant blue (CBB) staining (bottom). (C) GST-Rad9 and GST-Crk (120-225) were incubated with recombinant c-Abl in the presence or absence of 50 nM STI-571. The reaction products were analyzed by SDS-PAGE and autoradiography. (D) 293T cells were cotransfected with 3 μg of c-Abl or c-Abl(K-R) and GFP-Rad9 or GFP-Rad9(Y28-F). Anti-GFP immunoprecipitates (IP) were analyzed by immunoblotting (IB) with anti-P-Tyr (top) or anti-GFP (middle). Cell lysates were also subjected to immunoblotting with anti-c-Abl (bottom). Levels of c-Abl expression were quantitated by densitometric scanning of the signals.

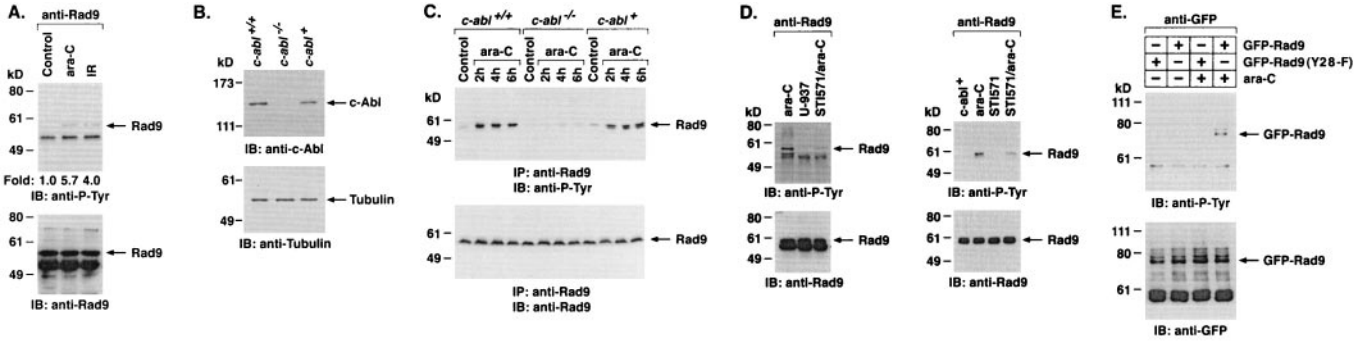

FIG. 4. c-Abl-dependent phosphorylation of Rad9 in response to DNA damage. (A) U-937 cells were treated with 10 μM ara-C or 15 Gy of IR and collected at 2 h. Anti-Rad9 immunoprecipitates were analyzed by immunoblotting (IB) with anti-P-Tyr (top) or anti-Rad9 (lower panel). Levels of Rad9 phosphorylation were quantitated by densitometric scanning of the signals. (B) c-*abl*$^{+/+}$, c-*abl*$^{-/-}$, and c-*abl*$^{+}$ cells were analyzed by immunoblotting with anti-c-Abl (top) or antitubulin (bottom). (C) c-*abl*$^{+/+}$, c-*abl*$^{-/-}$, and c-*abl*$^{+}$ cells were treated with 10 μM ara-C for the indicated times. Anti-Rad9 immunoprecipitates (IP) were analyzed by immunoblotting with anti-P-Tyr (top) or anti-Rad9 (bottom). (D) U-937 (left) and c-*abl*$^{+}$ (right) cells were left untreated or treated with 1 μM STI-571 for 24 h followed by treatment with 10 μM ara-C for 2 h. Anti-Rad9 immunoprecipitates were analyzed by immunoblotting with anti-P-Tyr (top) or anti-Rad9 (bottom). (E) 293T cells were transfected with 3 μg of GFP-Rad9 or GFP-Rad9(Y28-F) and treated with 10 μM ara-C for 2 h. Anti-GFP immunoprecipitates were analyzed by immunoblotting with anti-P-Tyr (top) or anti-GFP (bottom).

tion (46, 60). The finding that mutation of Rad9 Y28 to F completely inhibits c-Abl-mediated phosphorylation indicates that Y28 is the major c-Abl site (Fig. 3B, left). Moreover, the finding that c-Abl phosphorylates Rad9 but not Rad9 (1-265) indicates that binding to the C terminus is necessary for phosphorylation of the Y28 site (Fig. 3B, right). As confirmation that the phosphorylation of Rad9 is mediated by c-Abl, other studies were performed in the presence of c-Abl inhibitor STI-571 (11). The results demonstrate that STI-571 inhibits phosphorylation of Rad9 (Fig. 3C). To determine whether c-Abl phosphorylates Rad9 in vivo, kinase-active c-Abl or kinase-inactive c-Abl(K-R) was coexpressed with GFP-Rad9. Analysis of anti-GFP immunoprecipitates by immunoblotting with anti-P-Tyr demonstrated c-Abl-dependent tyrosine phosphorylation of Rad9 (Fig. 3D). As a control, there was little if any c-Abl-mediated phosphorylation of the Rad9(Y28-F) mutant (Fig. 3D). These findings demonstrate that the Rad9 Y28 site is required for c-Abl phosphorylation in vitro and in vivo.

DNA damage induces tyrosine phosphorylation of Rad9 by a c-Abl-dependent mechanism. To determine whether endogenous Rad9 is phosphorylated on tyrosine in cells, anti-Rad9 immunoprecipitates were analyzed by immunoblotting with anti-P-Tyr. The results demonstrate that treatment of cells with ara-C was associated with induction of Rad9 phosphorylation on tyrosine (Fig. 4A). ara-C incorporates into elongating DNA strands, inhibits DNA replication, and induces DNA double-strand breaks (13, 31, 36). The finding that exposure of cells to IR also induces tyrosine phosphorylation of Rad9 confirmed that this response is activated by genotoxic stress (Fig. 4A). To assess whether DNA damage induces tyrosine phosphorylation of Rad9 by a c-Abl-dependent mechanism, c-*abl*$^{+/+}$, c-*abl*$^{-/-}$, and c-*abl*$^{+}$ MEFs (Fig. 4B) (23) were treated with ara-C. Immunoblot analysis of anti-Rad9 immunoprecipitates with anti-P-Tyr demonstrated ara-C-induced tyrosine phosphorylation of Rad9 in c-*abl*$^{+/+}$ and c-*abl*$^{+}$ MEFs (Fig. 4C). By contrast, there was no detectable tyrosine phosphorylation of Rad9 in ara-C-treated c-*abl*$^{-/-}$ MEFs (Fig. 4C). To confirm that Rad9 is phosphorylated by c-Abl, U-937 cells were treated with STI-571 and then ara-C. Immunoblot analysis of anti-Rad9 immunoprecipitates with anti-P-Tyr demonstrated that STI-571 inhibits tyrosine phosphorylation of Rad9 (Fig. 4D, left). Similar findings were obtained with c-*abl*$^{+}$ cells (Fig. 4D, right). To determine whether Rad9 is phosphorylated on Y28 in response to DNA damage, cells expressing GFP-Rad9 or GFP-Rad9(Y28-F) were treated with ara-C (Fig. 4E). Anti-GFP immunoprecipitates were analyzed by immunoblotting with anti-P-Tyr. The demonstration that ara-C induces tyrosine phosphorylation of GFP-Rad9 but not GFP-Rad9(Y28-F) supported the specificity of the Y28 site (Fig. 4E). These findings demonstrate that Rad9 is phosphorylated on Y28 by a c-Abl-dependent mechanism in response to genotoxic stress.

c-Abl-mediated phosphorylation of Rad9 induces binding of Rad9 to Bcl-x_L. Recent studies have demonstrated that Rad9 binds to Bcl-2 and Bcl-x_L and that these interactions are dependent on the Rad9 BH3 domain (26, 27). To determine whether c-Abl-mediated phosphorylation of the Rad9 BH3 domain regulates the association of Rad9 and Bcl-x_L in vitro, GST-Rad9 was first incubated with c-Abl and ATP. Incubation of the reaction products with His–Bcl-x_L and analysis of products of adsorption to glutathione beads by immunoblotting with anti-Bcl-x_L demonstrated that c-Abl induces binding of Rad9 to Bcl-x_L (Fig. 5A). By contrast, c-Abl had no detectable effect on the association of Rad9(Y28-F) and Bcl-x_L (Fig. 5A). To extend this analysis, GST-Rad9 was incubated with c-Abl or c-Abl(K-R) and then assayed for binding to Bcl-x_L. The results show that c-Abl, and not c-Abl(K-R), induces the formation of Rad9–Bcl-x_L complexes (Fig. 5B). As an additional control, GST-Rad9 (1-265) was incubated with c-Abl or c-Abl(K-R). In agreement with the finding that Rad9 (1-265) is not phosphorylated by c-Abl (Fig. 3B), the binding of Rad9 (1-265) to Bcl-x_L was unaffected by c-Abl or c-Abl(K-R) (Fig. 5B). In in vivo studies, the association of Rad9 and Bcl-x_L was induced in cells expressing c-Abl (Fig. 5C). In agreement with the in vitro findings, c-Abl(K-R) had no detectable effect on the association of Rad9 and Bcl-x_L in cells (Fig. 5C). Moreover, c-Abl had

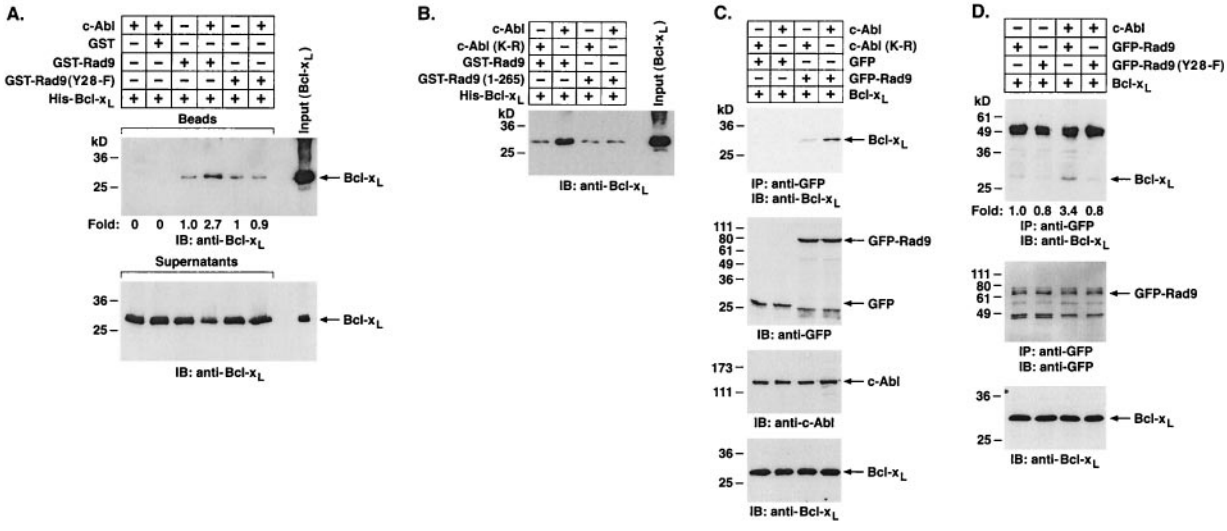

FIG. 5. Tyrosine phosphorylation of Rad9 by c-Abl induces binding of Rad9 to Bcl-x_L in vitro. (A) Glutathione beads containing GST, GST-Rad9, or GST-Rad9(Y28-F) were incubated with or without recombinant c-Abl and ATP for 30 min. The reaction mixtures were incubated with purified His–Bcl-x_L protein for an additional 1 h. The beads (top) and supernatants (bottom) were analyzed by SDS-PAGE and immunoblotting (IB) with anti-Bcl-x_L. Levels of Bcl-x_L binding to GST-Rad9 were quantitated by densitometric scanning of signals. (B) Recombinant c-Abl and c-Abl(K-R) were incubated with GST-Rad9 or GST-Rad9 (1-265) for 30 min followed by incubation with the purified His–Bcl-x_L protein for 1 h. Reaction products were separated by SDS-PAGE and analyzed by immunoblotting with anti-Bcl-x_L. (C) 293T cells were cotransfected with 1 μg of pcDNA3-Bcl-x_L and 3 μg of c-Abl, c-Abl(K-R), GFP vector, or GFP-Rad9. Anti-GFP immunoprecipitates (IP) were subjected to immunoblotting with anti-Bcl-x_L (top). Cell lysates were also subjected to immunoblotting with anti-GFP (second from top), anti-c-Abl (third from top), or anti-Bcl-x_L (bottom). (D) 293T cells were cotransfected with 1 μg of pcDNA3-Bcl-x_L and 3 μg of c-Abl, GFP-Rad9, or GFP-Rad9(Y28-F). Anti-GFP immunoprecipitates were subjected to immunoblotting with anti-Bcl-x_L (top) or anti-GFP (middle). Cell lysates were also subjected to immunoblotting with anti-Bcl-x_L (lower). Levels of Bcl-x_L binding to GFP-Rad9 were quantitated by densitometric scanning of the signals.

no detectable effect on the association of Rad9(Y28-F) and Bcl-x_L in cells (Fig. 5D).

Whereas the results demonstrate that Rad9 is phosphorylated by c-Abl in response to DNA damage and that c-Abl induces the binding of Rad9 and Bcl-x_L, studies were performed on U-937 cells expressing Bcl-x_L. Analysis of nuclear lysates from U-937/Bcl-x_L cells demonstrated cosedimentation of Rad9 and Bcl-x_L (Fig. 6A). Constitutive binding of Rad9

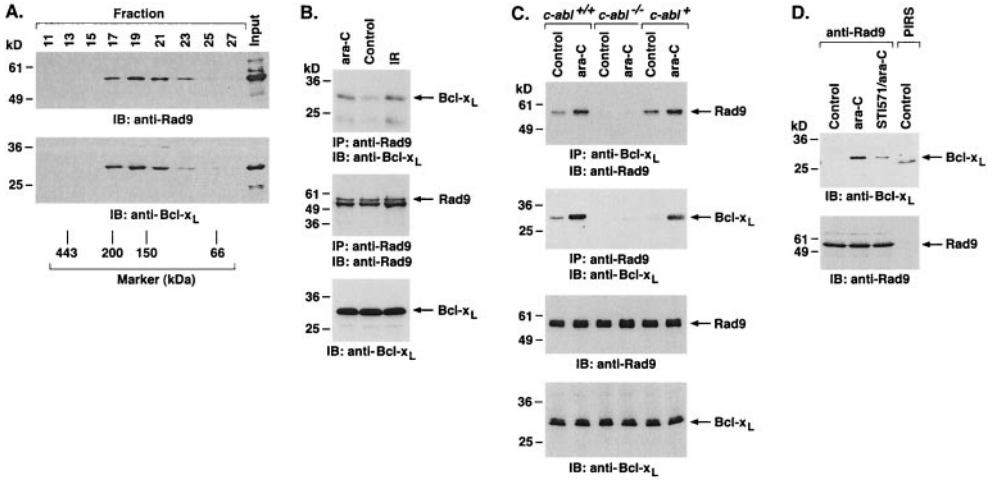

FIG. 6. DNA damage-induced binding of Rad9 to Bcl-x_L is a c-Abl-dependent mechanism. (A) Nuclear extracts from U-937/Bcl-x_L cells were layered onto a 10 to 35% glycerol gradient. After fractionation, the indicated fractions were subjected to SDS-PAGE and immunoblotting (IB) with anti-Rad9 (top) or anti-Bcl-x_L (bottom). (B) U-937/Bcl-x_L cells were treated with 10 μM ara-C or 15 Gy of IR for 2 h. Anti-Rad9 immunoprecipitates (IP) were analyzed by immunoblotting with anti-Bcl-x_L (top) or anti-Rad9 (middle). Cell lysates were also analyzed by immunoblotting with anti-Bcl-x_L (bottom). (C) c-$abl^{+/+}$, c-$abl^{-/-}$, and c-abl^{+} cells were treated with 10 μM ara-C for 2 h. Cell lysates were immunoprecipitated with anti-Bcl-x_L (top) or anti-Rad9 (second from top). The immunoprecipitates were subjected to immunoblotting with the indicated antibodies. Cell lysates were also subjected to immunoblotting with anti-Rad9 and anti-Bcl-x_L (bottom two blots). (D) c-abl^{+} cells were left untreated or were treated with 1 μM STI-571 for 24 h and then exposed to 10 μM ara-C for 2 h. Anti-Rad9 and preimmune rabbit serum (PIRS) immunoprecipitates were analyzed by immunoblotting with anti-Bcl-x_L (top) or anti-Rad9 (bottom).

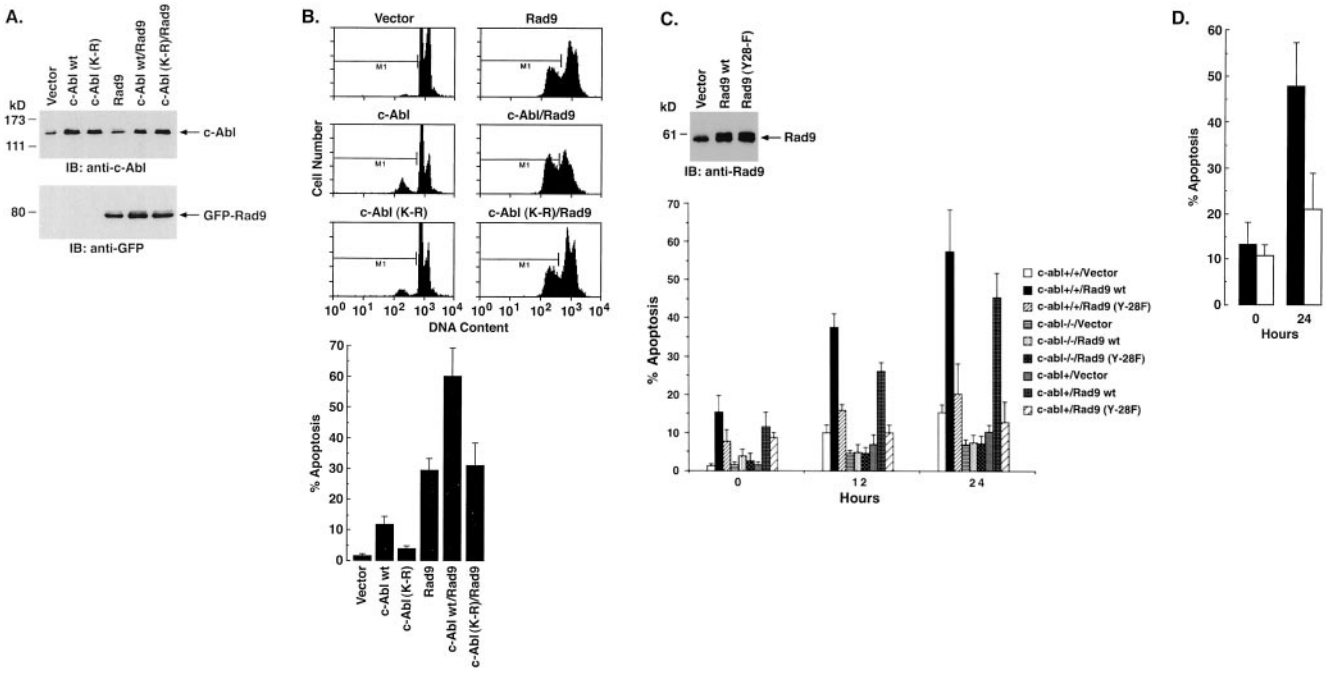

FIG. 7. c-Abl regulates Rad9-induced apoptosis in response to DNA damage. (A and B) 293T cells were transfected with 3 μg of c-Abl, c-Abl(K-R), or GFP-Rad9. (A) At 36 h posttransfection, cell lysates were subjected to immunoblot (IB) analysis with anti-c-Abl (top) or anti-GFP (bottom). (B) Cells were also fixed in ethanol and stained with propidium iodide. DNA content was analyzed by flow cytometry. The results (means ± standard deviations [SD] of two experiments, each performed in duplicate) are presented as the percentages of cells with sub-G_1 DNA. (C) c-*abl*$^{+/+}$, c-*abl*$^{-/-}$, and c-*abl*$^{+}$ cells were infected with a vector control or retrovirus vectors expressing Rad9 or Rad9(Y28-F). At 24 h postinfection, cell lysates were subjected to immunoblot analysis with anti-Rad9 (top). Infection efficiency as determined with pLXSN-GFP was 74.8% ± 3.6% (mean ± SD of three independent experiments). At 24 h postinfection, cells were left untreated or treated with 10 μM ara-C for 12 h and 24 h. The results (means ± SD of three independent experiments) are presented as the percentage of apoptotic cells with sub-G_1 DNA (bottom). wt, wild type. (D) c-*abl*$^{+}$ cells were left untreated (solid bar) or treated with 1 μM STI-571 (open bar) for 24 h and then exposed 10 μM ara-C for 24 h. The results (means ± SD) of three independent experiments are presented as the percentages of apoptotic cells with sub-G_1 DNA.

and Bcl-x_L was confirmed by immunoblot analysis of anti-Rad9 immunoprecipitates with anti-Bcl-x_L (Fig. 6B). Importantly, the constitutive association of Rad9 and Bcl-x_L was increased by ara-C treatment (Fig. 6B). Similar results were obtained with IR-treated cells (Fig. 6B). To further define the role of c-Abl in regulating the interaction of Rad9 and Bcl-x_L, lysates from ara-C-treated c-*abl*$^{+/+}$, c-*abl*$^{-/-}$, and c-*abl*$^{+}$ cells were subjected to immunoprecipitation with anti-Rad9. Analysis of the precipitates by immunoblotting with anti-Bcl-x_L demonstrated that DNA damage-induced formation of Rad9–Bcl-x_L complexes is mediated by a c-Abl-dependent mechanism (Fig. 6C). In agreement with these results, pretreatment of c-*abl*$^{+}$ cells with STI-571 blocked ara-C-induced formation of Rad9–Bcl-x_L complexes (Fig. 6D). These findings collectively indicate that c-Abl-mediated phosphorylation of the Rad9 BH3 domain induces binding of Rad9 to Bcl-x_L.

c-Abl potentiates Rad9-mediated apoptosis. To further assess the functional significance of the interaction between c-Abl and Rad9, 293T cells were transfected to express Rad9 and c-Abl or c-Abl(K-R) (Fig. 7A). The results demonstrate that c-Abl, and not c-Abl(K-R), potentiates the effects of Rad9 on the induction of 293 cell apoptosis (Fig. 7B). To extend this analysis, c-*abl*$^{+/+}$, c-*abl*$^{-/-}$, and c-*abl*$^{+}$ MEFs were infected with an empty retrovirus vector or one that expresses Rad9 (Fig. 7C). The apoptotic response of c-*abl*$^{+/+}$ and c-*abl*$^{+}$ MEFs to Rad9 was more pronounced than that obtained with c-*abl*$^{-/-}$ cells (Fig. 7C; 0 h). c-*abl*$^{+/+}$ and c-*abl*$^{+}$ MEFs expressing Rad9 also responded to ara-C treatment (Fig. 7C, 12 and 24 h) with a greater induction of apoptosis than that found with c-*abl*$^{-/-}$ cells expressing Rad9 (Fig. 7C). Moreover, expression of Rad9(Y28-F) was associated with attenuation of the apoptotic responses found with Rad9 (Fig. 7C). In agreement with these results, pretreatment of c-*abl*$^{+}$ cells with STI-571 inhibited Rad9-induced apoptosis (Fig. 7D). These results support a functional interaction between c-Abl and Rad9 that contributes to the induction of apoptosis.

DISCUSSION

Role of c-Abl in the apoptotic response to genotoxic stress. The mechanisms by which DNA damage is converted into intracellular signals that control cell behavior are largely unknown. Certain insights have been derived from the finding that the c-Abl tyrosine kinase is activated by agents that arrest DNA replication (e.g., ara-C) or induce DNA lesions (e.g., IR) (20, 23). The available evidence indicates that c-Abl functions in diverse aspects of the DNA damage response, including the activation of cell death signals. For example, transient transfection studies have demonstrated that wild-type c-Abl, but not kinase-inactive c-Abl(K-R), induces an apoptotic response (55). In addition, cells that stably express c-Abl(K-R) exhibit resistance to induction of apoptosis by ara-C and IR (16, 55).

These studies and the present work, which employs ectopic expression to assess function, can result in overinterpretation of findings. Similar results have nonetheless been obtained with c-*abl*$^{-/-}$ fibroblasts, although the apoptosis-resistant phenotype is more pronounced in cells expressing c-Abl(K-R) than in c-Abl null cells (16, 55). These findings indicate that a redundant function, perhaps mediated by the related Arg kinase (30), is inhibited by the dominant-negative effect of c-Abl(K-R).

Exposure of diverse mammalian cells to ara-C, IR, and other DNA-damaging agents is associated with activation of c-Abl and SAPK (8, 20, 23, 49). The demonstration that c-Abl-deficient cells exhibit a defective SAPK response to DNA damage has supported a role for c-Abl in regulation of the SAPK pathway (20, 23). More recent work has shown that c-Abl interacts directly with MEK kinase 1, an upstream effector of the SEK1→SAPK pathway, in response to DNA damage (22). In agreement with these findings, other studies have demonstrated that transient overexpression of activated forms of Abl stimulates SAPK activity (39, 41, 42). The functional significance of c-Abl-induced SAPK activation in the DNA damage response is supported by the demonstration that SAPK translocates to mitochondria and associates with the Bcl-x_L protein (24). SAPK phosphorylates Bcl-x_L on Thr-47 and Thr-115 and thereby contributes to the induction of apoptosis (24). In the present studies, we provide evidence that c-Abl also targets Bcl-x_L by a mechanism involving activation of Rad9.

c-Abl phosphorylates Rad9. In human cells, hRad9 forms a ternary complex with hRad1 and hHus1 (45, 50). The findings that hRad9 and hHus1 interact with the proliferating nuclear cell antigen suggested that the Rad9 complex contributes to the coordination of cell cycle progression, DNA replication, and DNA repair (28). Although few insights regarding the regulation of hRad9 are available, multiple phosphorylated forms of hRad9 have been detected in complexes with hRad1 and hHus1 (45). The kinases responsible for the modification of hRad9 and the functional significance of this regulation are unknown.

The present studies show that c-Abl binds directly to Rad9 and phosphorylates Rad9 on Y28 in vitro and in cells. The results also demonstrate that Rad9 is subject to c-Abl-mediated phosphorylation on Y28 in cells treated with genotoxic agents. Moreover, treatment of cells with 1 μM STI-571 partially inhibited phosphorylation of Rad9 on tyrosine. In agreement with these findings, activation of c-Abl in the DNA damage response is partially inhibited with 1 μM STI-571 and completely inhibited with 10 μM STI-571 (data not shown). Thus, inhibition of DNA replication by ara-C treatment or induction of DNA lesions by IR exposure induces tyrosine phosphorylation of Rad9 by a c-Abl-dependent mechanism. Rad9 contains a motif of 15 amino acids near the N terminus (amino acids 15 to 30) that includes conserved residues found in BH3 domains of proapoptotic Bcl-2 family members (27). The BH3 domain-only proteins function as transdominant inhibitors by binding to antiapoptotic members of the Bcl-2 family and blocking their survival function (1, 18). Notably, Y28 resides in the Rad9 BH3 domain. Moreover, the Rad9 Y28 site is unique to BH3 consensus sequences found in other proapoptotic members of the Bcl-2 family. These findings support a model in which c-Abl-mediated phosphorylation of the Rad9 BH3 domain is selective for this proapoptotic member of the Bcl-2 family.

c-Abl regulates the interaction between hRad9 and Bcl-x_L. We have previously shown that the Rad9 BH3 domain regulates the interaction of Rad9 with the antiapoptotic Bcl-2 and Bcl-x_L proteins (27). The present results demonstrate that c-Abl-mediated phosphorylation of Rad9 on Y28 induces the interaction of Rad9 and Bcl-x_L. In vitro studies show that Rad9 associates constitutively with Bcl-x_L and that c-Abl stimulates this interaction. By contrast, c-Abl had no effect on constitutive binding of Rad9(Y28-F) to Bcl-x_L. In transfected cells, c-Abl also increased the interaction of Rad9, but not of Rad9(Y28-F), with Bcl-x_L. In agreement with these results, exposure of cells to agents, such as ara-C and IR, that activate c-Abl (20, 23) was associated with binding of Rad9 to Bcl-x_L. By contrast, results obtained with c-Abl-deficient cells or after treatment of wild-type cells with STI-571 indicate that c-Abl has little if any effect on the binding of Rad9 to Rad1 and Hus1 in response to DNA damage (data not shown). The finding that DNA damage induces the interaction between Rad9 and Bcl-x_L in c-*abl*$^{+/+}$ and c-*abl*$^{+}$, but not in c-*abl*$^{-/-}$, cells further indicated that this response is c-Abl dependent.

Nuclear magnetic resonance and X-ray crystallographic analysis of the Bcl-x_L monomer has demonstrated that the α-helices of BH1 to -3 form a hydrophobic pocket (35). The BH3 amphipathic α2-helix of proapoptotic family members is essential for binding to the pocket and for inhibition of Bcl-x_L function (43, 51, 59). The present results support a model in which modification of the Rad9 BH3 α-helix by c-Abl-mediated phosphorylation is associated with a structural change that facilitates binding to the Bcl-x_L hydrophobic pocket. Other studies have demonstrated that c-Abl functions upstream of SAPK-mediated phosphorylation of Bcl-x_L (24). SAPK phosphorylates Bcl-x_L on (i) Thr-47, which resides in the loop between the α1- and α2-helices, and (ii) Thr-115, which is adjacent to the α3-helix (24). The demonstration that the Bcl-x_L(A-47,-115) mutant is more effective than wild-type Bcl-x_L in blocking apoptosis indicates that phosphorylation of Thr-47 and Thr-115 is involved in regulating Bcl-x_L function (24). These findings suggest that modifications of both the Rad9 BH3 domain by c-Abl and of Bcl-x_L directly by SAPK are involved in regulating the function of Bcl-x_L in protecting against apoptosis.

c-Abl potentiates the proapoptotic function of Rad9. The results of the present study demonstrate that Rad9-induced apoptosis is potentiated by expression of c-Abl and not by the kinase-inactive c-Abl(K-R) mutant. As c-Abl interacts with multiple targets that may contribute to DNA damage-induced apoptosis (25), we performed studies to assess the contribution of the c-Abl–Rad9 interaction to this response. The demonstration that expression of Rad9 and that of Rad9(Y28-F) in cells are associated with similar levels of apoptosis indicated that mutation of Y28 has no apparent effect on Rad9's basal proapoptotic function. By contrast, the results show that DNA damage-induced apoptosis is potentiated by expression of Rad9 and not by that of Rad9(Y28-F). In addition, Rad9-mediated induction of apoptosis in response to DNA damage was attenuated in c-Abl-deficient cells. These findings collectively support a model in which c-Abl-mediated phosphorylation of Rad9 in the DNA damage response contributes to the

binding of Rad9 to Bcl-x_L and thereby to potentiation of Rad9-induced apoptosis.

ACKNOWLEDGMENTS

This work was supported by grants CA29431 and CA55241 awarded by the National Cancer Institute.

We thank R. Ren and D. Baltimore for providing the c-*abl*$^{-/-}$ and c-*abl*$^{+}$ fibroblast cell lines. We appreciate the helpful discussions with Jun-ichi Sawada and the technical assistance of Kamal Chauhan.

REFERENCES

1. **Adams, J. M., and S. Cory.** 1998. The Bcl-2 protein family: arbiters of cell survival. Science **281:**1322–1326.
2. **Agami, R., G. Blandino, M. Oren, and Y. Shaul.** 1999. Interaction of c-Abl and p73α and their collaboration to induce apoptosis. Nature **399:**809–813.
3. **al-Khodairy, F., and A. M. Carr.** 1992. DNA repair mutants defining G_2 checkpoint pathways in Schizosaccharomyces pombe. EMBO J. **11:**1343–1350.
4. **al-Khodairy, F., E. Fotou, K. S. Sheldrick, D. J. Griffiths, A. R. Lehmann, and A. M. Carr.** 1994. Identification and characterization of new elements inv olved in checkpoint and feedback controls in fission yeast. Mol. Biol. Cell **5:**147–160.
5. **Baskaran, R., L. D. Wood, L. L. Whitaker, Y. Xu, C. Barlow, C. E. Canman, S. E. Morgan, D. Baltimore, A. Wynshaw-Boris, M. B. Kastan, and J. Y. J. Wang.** 1997. Ataxia telangiectasia mutant protein activates c-abl tyrosine kinase in response to ionizing radiation. Nature **387:**516–519.
6. **Bessho, T., and A. Sancar.** 2000. Human DNA damage checkpoint protein hRAD9 is a 3′ to 5′ exonuclease. J. Biol. Chem. **275:**7451–7454.
7. **Burtelow, M. A., S. H. Kaufmann, and L. M. Karnitz.** 2000. Retention of the human Rad9 checkpoint complex in extraction-resistant nuclear complexes after DNA damage. J. Biol. Chem. **275:**26343–26348.
8. **Chen, Y.-R., X. Wang, D. Templeton, R. J. Davis, and T.-H. Tan.** 1996. The role of c-Jun N-terminal kinase (JNK) in apoptosis induced by ultraviolet C and γ radiation. J. Biol. Chem. **271:**31929–31936.
9. **Datta, R., Y. Manome, N. Taneja, L. H. Boise, R. R. Weichselbaum, C. B. Thompson, C. A. Slapak, and D. W. Kufe.** 1995. Overexpression of Bcl-x_L by cytotoxic drug exposure confers resistance to ionizing radiation-induced internucleosomal DNA fragmentation. Cell Growth Differ. **6:**363–370.
10. **Dignam, J. D., R. M. Lebovitz, and R. G. Roeder.** 1983. Accurate transcription initiation by RNA polymerase II in a soluble extract from isolated mammalian nuclei. Nucleic Acids Res. **11:**1475–1489.
11. **Druker, B. J., S. Tamura, E. Buchdunger, S. Ohno, G. M. Segal, S. Fanning, J. Zimmermann, and N. B. Lydon.** 1996. Effects of a selective inhibitor of the Abl tyrosine kinase on the growth of Bcr-Abl positive cells. Nat. Med. **2:**561–566.
12. **Feller, S. M., B. Knudsen, and H. Hanafusa.** 1994. c-Abl kinase regulates the protein binding activity of c-Crk. EMBO J. **13:**2341–2351.
13. **Fram, R. J., and D. Kufe.** 1982. DNA strand breaks caused by inhibitors of DNA synthesis: 1-β-D-arabinofuranosylcytosine and aphidicolin. Cancer Res. **42:**4050–4053.
14. **Freire, R., J. R. Murguia, M. Tarsounas, N. F. Lowndes, P. B. Moens, and S. P. Jackson.** 1998. Human and mouse homologs of Schizosaccharomyces pombe rad1(+) and Saccharomyces cerevisiae RAD17: linkage to checkpoint control and mammalian meiosis. Genes Dev. **12:**2560–2573.
15. **Gong, J., A. Costanzo, H. Yang, G. Melino, W. Kaelin, Jr., M. Levrero, and J. Y. J. Wang.** 1999. The tyrosine kinase c-Abl regulates p73 in apoptotic response to cisplatin-induced DNA damage. Nature **399:**806–809.
16. **Huang, Y., Z. M. Yuan, T. Ishiko, S. Nakada, T. Utsugisawa, T. Kato, S. Kharbanda, and D. W. Kufe.** 1997. Pro-apoptotic effect of the c-Abl tyrosine kinase in the cellular response to 1-β-D-arabinofuranosylcytosine. Oncogene **15:**1947–1952.
17. **Jin, S., S. Kharbanda, B. Mayer, D. Kufe, and D. T. Weaver.** 1997. Binding of Ku and c-Abl at the kinase homology region of DNA-dependent protein kinase catalytic subunit. J. Biol. Chem. **272:**24763–24766.
18. **Kelekar, A., and C. B. Thompson.** 1998. Bcl-2-family proteins: the role of the BH3 domain in apoptosis. Trends Cell Biol. **8:**324–330.
19. **Kharbanda, S., P. Pandey, S. Jin, S. Inoue, A. Bharti, Z.-M. Yuan, R. Weichselbaum, D. Weaver, and D. Kufe.** 1997. Functional interaction of DNA-PK and c-Abl in response to DNA damage. Nature **386:**732–735.
20. **Kharbanda, S., P. Pandey, R. Ren, S. Feller, B. Mayer, L. Zon, and D. Kufe.** 1995. c-Abl activation regulates induction of the SEK1/stress activated protein kinase pathway in the cellular response to 1-β-D-arabinofuranosylcytosine. J. Biol. Chem. **270:**30278–30281.
21. **Kharbanda, S., P. Pandey, L. Schofield, S. Israels, R. Roncinske, K. Yoshida, A. Bharti, Z. Yuan, S. Saxena, R. Weichselbaum, C. Nalin, and D. Kufe.** 1997. Role for Bcl-x_L as an inhibitor of cytosolic cytochrome C accumulation in apoptosis. Proc. Natl. Acad. Sci. USA **94:**6939–6942.
22. **Kharbanda, S., P. Pandey, T. Yamauchi, S. Kumar, M. Kaneki, V. Kumar, A. Bharti, Z. Yuan, L. Ghanem, A. Rana, R. Weichselbaum, G. Johnson, and D. Kufe.** 2000. Activation of MEK kinase-1 by the c-Abl protein tyrosine kinase in response to DNA damage. Mol. Cell. Biol. **20:**4979–4989.
23. **Kharbanda, S., R. Ren, P. Pandey, T. D. Shafman, S. M. Feller, R. R. Weichselbaum, and D. W. Kufe.** 1995. Activation of the c-Abl tyrosine kinase in the stress response to DNA-damaging agents. Nature **376:**785–788.
24. **Kharbanda, S., S. Saxena, K. Yoshida, P. Pandey, M. Kaneki, Q. Wang, K. Cheng, Y. Chen, A. Campbell, S. Thangrila, Z. Yuan, J. Narula, R. Weichselbaum, C. Nalin, and D. Kufe.** 2000. Translocation of SAPK/JNK to mitochondria and interaction with Bcl-x_L in response to DNA damage. J. Biol. Chem. **275:**322–327.
25. **Kharbanda, S., Z. Yuan, R. Weichselbaum, and D. Kufe.** 1998. Determination of cell fate by c-Abl activation in the response to DNA damage. Oncogene **17:**3309–3318.
26. **Komatsu, K., K. M. Hopkins, H. B. Lieberman, and H. Wang.** 2000. Schizosaccharomyces pombe Rad9 contains a BH3-like region and interacts with the anti-apoptotic protein Bcl-2. FEBS Lett. **481:**122–126.
27. **Komatsu, K., T. Miyashita, H. Hang, K. M. Hopkins, W. Zheng, S. Cuddeback, M. Yamada, H. B. Lieberman, and H. G. Wang.** 2000. Human homologue of S. pombe Rad9 interacts with BCL-2/BCL-xL and promotes apoptosis. Nat. Cell Biol. **2:**1–6.
28. **Komatsu, K., W. Wharton, H. Hang, C. Wu, S. Singh, H. Lieberman, W. Pledger, and H. Wang.** 2000. PCNA interacts with hHus1/hRad9 in response to DNA damage and replication inhibition. Oncogene **19:**5291–5297.
29. **Kostrub, C. F., K. Knudsen, S. Subramani, and T. Enoch.** 1998. Hus1p, a conserved fission yeast checkpoint protein, interacts with Rad1p and is phosphorylated in response to DNA damage. EMBO J. **17:**2055–2066.
30. **Kruh, G. D., R. Perego, T. Miki, and S. A. Aaronson.** 1990. The complete coding sequence of arg defines the Abelson subfamily of cytoplasmic tyrosine kinases. Proc. Natl. Acad. Sci. USA **87:**5802–5806.
31. **Kufe, D. W., P. P. Major, E. M. Egan, and G. P. Beardsley.** 1980. Correlation of cytotoxicity with incorporation of ara-C into DNA. J. Biol. Chem. **255:**8997–9000.
32. **Lieberman, H. B., K. M. Hopkins, M. Nass, D. Demetrick, and S. Davey.** 1996. A human homolog of the Schizosaccharomyces pombe rad9+ checkpoint control gene. Proc. Natl. Acad. Sci. USA **93:**13890–13895.
33. **Mayer, B. J., and D. Baltimore.** 1994. Mutagenic analysis of the roles of SH2 and SH3 domains in regulation of the Abl tyrosine kinase. Mol. Cell. Biol. **14:**2883–2894.
34. **Miller, A. D., J. V. Garcia, N. von Suhr, C. M. Lynch, C. Wilson, and M. V. Eiden.** 1991. Construction and properties of retrovirus packaging cells based on gibbon ape leukemia virus. J. Virol. **65:**2220–2224.
35. **Muchmore, S. W., M. Sattler, H. Liang, R. P. Meadows, J. E. Harlan, H. S. Yoon, D. Nettesheim, B. S. Chang, C. B. Thompson, S.-L. Wong, S.-C. Ng, and S. W. Fesik.** 1996. X-ray and NMR structure of human Bcl-x_L, an inhibitor of programmed cell death. Nature **381:**335–341.
36. **Ohno, Y., D. Spriggs, A. Matsukage, T. Ohno, and D. Kufe.** 1988. Effects of 1-β-D-arabinofuranosylcytosine incorporation on elongation of specific DNA sequences by DNA polymerase β. Cancer Res. **48:**1494–1498.
37. **Pandey, P., J. Raingeaud, M. Kaneki, R. Weichselbaum, R. Davis, D. Kufe, and S. Kharbanda.** 1996. Activation of p38 MAP kinase by c-Abl-dependent and -independent mechanisms. J. Biol. Chem. **271:**23775–23779.
38. **Parker, A. E., I. van de Weyer, M. C. Laus, I. Oostveen, J. Yon, P. Verhasselt, and W. H. Luyten.** 1998. A human homologue of the Schizosaccharomyces pombe rad1+ checkpoint gene encodes an exonuclease. J. Biol. Chem. **273:**18332–18339.
39. **Raitano, A. B., J. R. Halpern, T. M. Hambuch, and C. L. Sawyers.** 1995. The Bcr-Abl leukemia oncogene activates Jun kinase and requires Jun for transformation. Proc. Natl. Acad. Sci. USA **92:**11746–11750.
40. **Ren, R., Z. Ye, and D. Baltimore.** 1994. Abl protein-tyrosine kinase selects the Crk adaptor as a substrate using SH3-binding sites. Genes Dev. **8:**783–795.
41. **Renshaw, M. W., E. Lea-Chou, and J. Y. J. Wang.** 1996. Rac is required for v-Abl tyrosine kinase to activate mitogenesis. Curr. Biol. **6:**76–83.
42. **Sanchez, Y., C. Wong, R. S. Thoma, R. Richman, Z. Wu, H. Piwnica-Worms, and S. J. Elledge.** 1997. Conservation of the Chk1 checkpoint pathway in mammals: linkage of DNA damage to Cdk regulation through Cdc25. Science **277:**1497–1501.
43. **Sattler, M., R. Salgia, K. Okuda, N. Uemura, M. A. Durstin, E. Pisick, G. Xu, J. L. Li, K. V. Prasad, and J. D. Griffin.** 1996. The proto-oncogene product p120BCR/ABL and the adaptor proteins CRKL and c-CRK link c-ABL, p190BCR/ABL and p210BCR/ABL to the phosphatidylinositol-3′ kinase pathway. Oncogene **12:**839–846.
44. **Shafman, T., K. K. Khanna, P. Kedar, K. Spring, S. Kozlov, T. Yen, K. Hobson, M. Gatei, N. Zhang, D. Watters, M. Egerton, Y. Shiloh, S. Kharbanda, D. Kufe, and M. F. Lavin.** 1997. Interaction between ATM protein and c-Abl in response to DNA damage. Nature **387:**520–523.
45. **St. Onge, R. P., C. M. Udell, R. Casselman, and S. Davey.** 1999. The human

G_2 checkpoint control protein hRAD9 is a nuclear phosphoprotein that forms complexes with hRAD1 and hHUS1. Mol. Biol. Cell **10:**1985–1995.
46. **Till, J. H., P. M. Chan, and W. T. Miller.** 1999. Engineering the substrate specificity of the Abl tyrosine kinase. J. Biol. Chem. **274:**4995–5003.
47. **Tybulewicz, V. L. J., C. E. Crawford, P. K. Jackson, R. T. Bronson, and R. C. Mulligan.** 1991. Neonatal lethality and lymphopenia in mice with a homozygous disruption of the c-abl proto-oncogene. Cell **65:**1153–1163.
48. **Udell, C. M., S. K. Lee, and S. Davey.** 1998. RAD1 and MRAD1 encode mammalian homologues of the fission yeast rad1(+) cell cycle checkpoint control gene. Nucleic Acids Res. **26:**3971–3976.
49. **Verheij, M., R. Bose, X. H. Lin, B. Yhao, W. D. Jarvis, S. Grant, M. J. Birrer, E. Szabo, L. I. Zon, J. M. Kyriakis, A. Haimovitz-Friedman, Z. Fuks, and R. N. Kolesnick.** 1996. Requirement for ceramide-initiated SAPK/JNK signalling in stress-induced apoptosis. Nature **380:**75–79.
50. **Volkmer, E., and L. M. Karnitz.** 1999. Human homologs of Schizosaccharomyces pombe rad1, hus1, and rad9 form a DNA damage-responsive protein complex. J. Biol. Chem. **274:**567–570.
51. **Wang, K., X. M. Yin, D. T. Chao, C. L. Milliman, and S. J. Korsmeyer.** 1996. BID: a novel BH3 domain-only death agonist. Genes Dev. **10:**2859–2869.
52. **Yoshida, K., S. Kharbanda, and D. Kufe.** 1999. Functional interaction between SHPTP1 and the Lyn tyrosine kinase in the apoptotic response to DNA damage. J. Biol. Chem. **274:**34663–34668.
53. **Yoshida, K., R. Weichselbaum, S. Kharbanda, and D. Kufe.** 2000. Role for the Lyn tyrosine kinase as a regulator of stress-activated protein kinase activity in response to DNA damage. Mol. Cell. Biol. **20:**5370–5380.
54. **Yuan, Z., Y. Huang, M. Fan, C. Sawers, S. Kharbanda, and D. Kufe.** 1996. Genotoxic drugs induce interaction of the c-Abl tyrosine kinase and the tumor suppressor protein p53. J. Biol. Chem. **271:**26457–26460.
55. **Yuan, Z., Y. Huang, T. Ishiko, S. Kharbanda, R. Weichselbaum, and D. Kufe.** 1997. Regulation of DNA damage-induced apoptosis by the c-Abl tyrosine kinase. Proc. Natl. Acad. Sci. USA **94:**1437–1440.
56. **Yuan, Z. M., Y. Huang, T. Ishiko, S. Nakada, T. Utsugisawa, S. Kharbanda, P. Sung, A. Shinohara, R. Weichselbaum, and D. Kufe.** 1998. Regulation of Rad51 function by c-Abl in response to DNA damage. J. Biol. Chem. **273:**3799–3802.
57. **Yuan, Z. M., Y. Huang, Y. Whang, C. Sawyers, R. Weichselbaum, S. Kharbanda, and D. Kufe.** 1996. Role for the c-Abl tyrosine kinase in the growth arrest response to DNA damage. Nature **382:**272–274.
58. **Yuan, Z. M., H. Shioya, T. Ishiko, X. Sun, Y. Huang, H. Lu, S. Kharbanda, R. Weichselbaum, and D. Kufe.** 1999. p73 is regulated by the c-Abl tyrosine kinase in the apoptotic response to DNA damage. Nature **399:**814–817.
59. **Zha, J., H. Harada, E. Yang, J. Jockel, and S. J. Korsmeyer.** 1996. Serine phosphorylation of death agonist BAD in response to survival factor results in binding to 14–3–3 not BCL-X_L. Cell **87:**619–628.
60. **Zhou, S., K. L. Carraway, M. J. Eck, S. C. Harrison, R. A. Feldman, M. Mohammadi, J. Schlessinger, S. R. Hubbard, D. P. Smith, and C. Eng.** 1995. Catalytic specificity of protein-tyrosine kinases is critical for selective signalling. Nature **373:**536–539.